J Comput Electron (2008) 7: 222–225
DOI 10.1007/s10825-008-0197-3

Semi-discrete 2D Wigner-particle approach

Mihail Nedjalkov · Dragica Vasileska

Published online: 26 January 2008
© Springer Science+Business Media LLC 2008

Abstract We suggest particle-based approach for simulation of carrier transport in 2D devices. The quantum character of the carrier transport is taken into account by generation and recombination of positive and negative particles. Preliminary applications of the approach are discussed. Also, a variety of issues are raised regarding many computational challenges that need to be overcome.

Keywords Wigner transport · Monte Carlo methods

1 The transport model

The Wigner function (WF) approach to device simulations is regarded as convenient, as it maintains many classical concepts describing evolution and dissipation processes, as well as discouraging, due to many open numerical and theoretical issues. Two decades ago the coherent 1D Wigner equation has been solved by deterministic approaches [1], which furthermore have been refined towards self-consistent schemes and dissipation processes using the relaxation time approximation. It has been recognized that an increase of the dimensions of the task is prohibited by an enormous increase of the memory requirements. Indeed, the experience with deterministic Boltzmann simulators can not be applied to the quantum counterpart since the matrix corresponding to the Wigner potential operator is dense. Recently two Monte Carlo methods for Wigner transport have been proposed [2, 3]. The first method, derived by an operator splitting approach, utilizes an ensemble of particles which carry the quantum information via a quantity called affinity. It originates from the Wigner potential, whose values are distributed between particles according to their phase space position. The viability of the method has been excellently demonstrated into a recent quasi two-dimensional simulations of double gate MOSFET's [4]. The second method is based on a formal application of the Monte Carlo theory on the integral form of the Wigner equation. The action of the Wigner potential is interpreted as generation of couples of positive and negative particles. The quantum information is carried by their sign, all other aspects of their evolution including the scattering by phonons are of usual Boltzmann picture. The avalanche of generated particles is controlled by the inverse process: two particles with opposite sign entering given phase space cell annihilate.

Here we examine the applicability of the second method to model realistic 2D transport problems. In this case the formulation of the transport equation can become semi-discrete in accordance with the following. Recent theoretical studies [5] show that the conventional WF formulation conflicts with the open system boundary conditions giving rise to unphysical effects. The problem is avoided if (i) the plane wave basis of the infinite Weyl-Wigner transform is replaced by a generic basis set [5]; (ii) the coherence integral of the transform is bounded inside the device by the assumption of vanishing correlation with the states in the leads [6]. Otherwise, the coherence length becomes a free numerical parameter, which affects the computed physical quantities.

To examine these results in 2D problems we consider a typical MOSFET structure schematically shown in Fig. 1. The device shape is a rectangle, the doped source and drain regions are marked in gray. To the left and right of the

M. Nedjalkov (✉)
Institute for Microelectronics, TU Wien, Gußhausstraße 27–29, 1040 Wien, Austria
e-mail: mixi@iue.tuwien.ac.at

D. Vasileska
Department of Electrical Engineering, Arizona State University, Tempe, AZ 85287-5706, USA

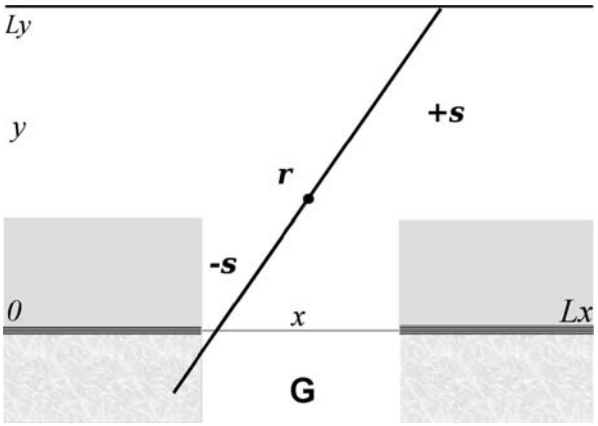

Fig. 1 A conventional 2D structure. The device is bounded by the rectangle L_y, 0, L_x. The correlation line penetrates into the left lead. The leads are implied by the shadowed regions on bot sides of the **G** region, where $y < 0$

gate region are shown parts of the leads. The latter specify the boundary conditions in the two tinny strips marked in black. It is assumed that the current flows between the device and the leads only, that is, at the rest of the device boundary including the region under the gate carriers are reflected. The states of the carriers are characterized by wave functions which become zero at and outside these boundaries. Accordingly the density matrix $\rho_t(\mathbf{r}_1, \mathbf{r}_2)$, will vanish if some of the arguments $\mathbf{r} = (x, y)$ is outside of the rectangle $(0, \mathbf{L}) = (0, L_x); (0, L_y)$ determined by the device dimensions, but on the leads. This restriction is raised if we assume that there is no correlation with the states in the leads. The Wigner function is obtained from the density matrix by the continuous Fourier transform of $\rho_t(\mathbf{r} + \frac{\mathbf{s}}{2}, \mathbf{r} - \frac{\mathbf{s}}{2}, t)$ where $\mathbf{r} = \frac{\mathbf{r}_1 + \mathbf{r}_2}{2}$ and $\mathbf{s} = \mathbf{r}_1 - \mathbf{r}_2$. The fact that ρ is confined gives rise to the following condition for $\mathbf{s}$: $-\mathbf{L}_c < \mathbf{s} < \mathbf{L}_c$, $\mathbf{L}_c = 2\min(\mathbf{r}, (\mathbf{L} - \mathbf{r}))$. In the spirit of (i) this allows to use the discrete Fourier basis corresponding to the rectangle. The quantity $\mathbf{L}_c(\mathbf{r})$ can be identified as the coherence length. In order to avoid the dependence on $\mathbf{r}$ it furthermore can be conveniently fixed to the maximal value of the above minimum: $\mathbf{L}_c = \mathbf{L}$. by formally including a domain indicator $\theta_D(\mathbf{s})$ in the definition.

Alternatively, if the leads must be taken into account we consider the line on Fig. 1. The segment of this line lying in the gate region (and the corresponding counterpart in the device) must be excluded from the correlation integral. The correlation is enabled after the point of entering into the leads. However, even in this case, $\mathbf{s}$ remains bounded, on the expense that $\mathbf{L}_c$ must be augmented to $(0, L_x); (-L_y, L_y)$. In this way the geometry of the chosen structure reduces the choice of the coherence length to two possible cases. By applying the discrete Fourier transform

$$f(\mathbf{r}, \mathbf{n}, t) = \frac{1}{\mathbf{L}_c} \int_{-\mathbf{L}_c/2}^{\mathbf{L}_c/2} d\mathbf{s} e^{i2\mathbf{n}\Delta\mathbf{k}\mathbf{s}} \rho_t(\mathbf{r}, \mathbf{s}); \quad \mathbf{n} = (n_x, n_y),$$

$$\rho_t(\mathbf{r}, \mathbf{s}) = \sum_{\mathbf{n}=-\infty}^{\infty} e^{i2\mathbf{n}\Delta\mathbf{k}\mathbf{s}} f(\mathbf{r}, \mathbf{n}, t); \quad \Delta\mathbf{k} = \pi/\mathbf{L}_c$$

to the von-Neumann equation for the density matrix we obtain a Wigner equation which is continuous in space and discrete in momentum: The equation has the usual form but a sum replaces the integral of the Wigner potential. We note the presence of the domain indicator in the definition of the latter:

$$\frac{1}{i\hbar} \frac{1}{\mathbf{L}_c} \int_{-\mathbf{L}_c/2}^{\mathbf{L}_c/2} d\mathbf{s} e^{-i2\mathbf{M}\Delta\mathbf{k}\mathbf{s}} (V(\mathbf{r} + \mathbf{s}) - V(\mathbf{r} - \mathbf{s}))\theta_D(\mathbf{s}). \quad (1)$$

According the particle sign approach [3], the Wigner potential generates particles with a frequency given by the Wigner out-scattering rate γ obtained from (1):

$$\gamma(\mathbf{r}) = \sum_{\mathbf{M}=0}^{\infty} |V_w(\mathbf{r}, \mathbf{M})|. \quad (2)$$

We note that the above considerations remain valid in the more general case accounting for phonon scattering. As the latter is inherent for particle methods, it is important to carefully develop and test the coherent approach.

2 Computational aspects

The first objective is to explore the convergence of the developed algorithm, which indicates whether the approach is in general numerically feasible.

A stationary case is considered, where the boundary conditions control the carrier transport. The algorithm is build on top of a standard MC simulator. Classical Ensemble MC simulations of the device under considerations provide the self-consistent potential. It provides for the Wigner particles the generation rate γ and the scattering probability table. The quantum ensemble is evolved in the phase space at consecutive time steps. An evolving particle gives rise to secondary, ternary etc. particles which are sequentially processed for the rest of the flight time step in the same way. As the entire potential is used in (2), the driving force is zero. Another feature is that Wigner particles are indistinguishable: Only their sign is accumulated in an array f of integers associated to grid points of a mesh in the phase space. The reason for this approach is the huge magnitude $\gamma \simeq [10^{15}/\mathrm{s}]$ of the generation rate, which does not allow individual treatment of the particles. The inverse process of particle annihilation occurs in the particular cells $\Delta\mathbf{r}$, $\Delta\mathbf{k}$ of decomposition of the real and wave vector subspaces. Due to this, each integer can be positive, zero or negative. Depending on the size of the device and the mesh, the array which actually corresponds to the Wigner function may easily contain 10^7 elements. After the evolution step particles

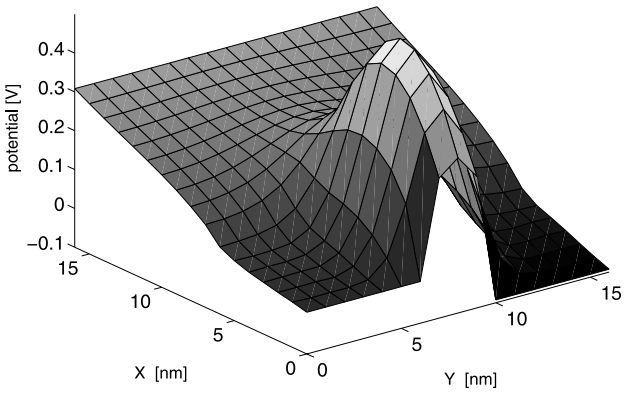

Fig. 2 Device potential

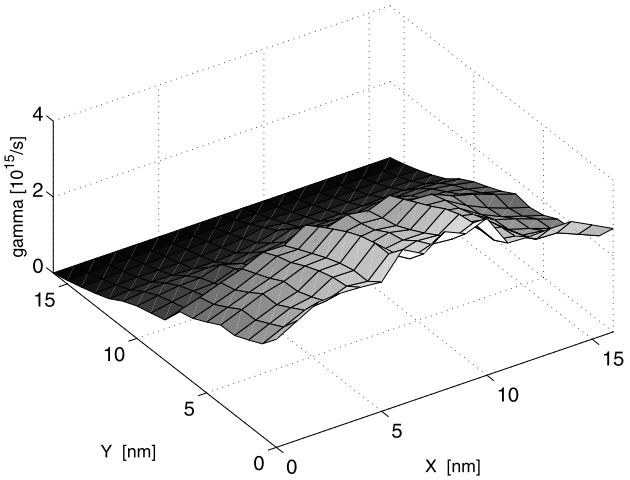

Fig. 3 Generation rate γ derived from the potential presented on Fig. 2

retain their wave vector value as the field is zero and the generation utilizes the same mesh. On the contrary, the position assignment is a large scale problem since the wave vector ranges over several orders of magnitude. For fast particles which cross several cells during the time step, the assignment introduces small error in the spatial evolution. More dramatic is the situation with the slow particles: if during the time step a particle crosses a distance less than a half of the mesh step it can remain around a grid point for a long time. This is an example for artificial diffusion which is treated in the following way: (i) Slow particles, e.g. these which belong to the cells around the zero are treated in a standard ensemble approach: the phase space evolution is followed continuously throughout the device. (ii) The grid assignment is chosen stochastically, according a probability proportional to the distance to the neighborhood grid points.

The presented simulation results aim to demonstrate the numerical features of the method and thus are qualitative. A model Γ valley semiconductor with 0.036 effective mass is chosen. Figure 2 shows the potential profile in a 16×16 nm device. The S/D regions are of 6 nm width

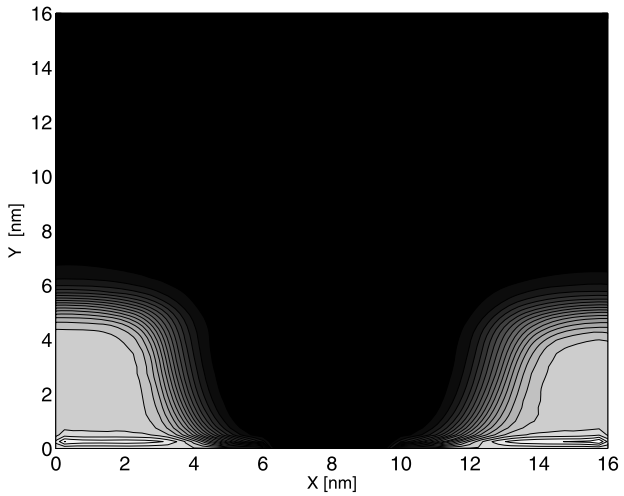

Fig. 4 Classical density. Carriers are distributed by the driving electrical force

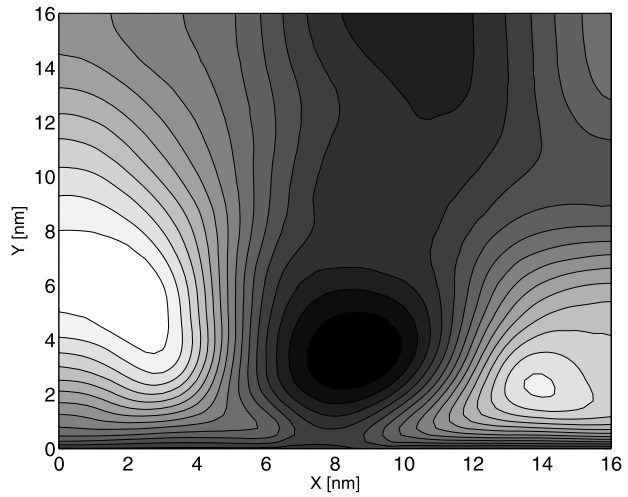

Fig. 5 Quantum density. The particle motion is inertial, the pattern is due to generation-annihilation processes only

and depth, the substrate is 10 nm. The 4 nm thick and 6 nm long barrier rapidly drops on both sides of the 0.45 V peak. Doping and bias values are selected in a way to give rise to a strong asymmetry in x and y directions. It is the central entity, selected to govern the quantum effects into a particular pattern. The generation rate, where the correlation in the leads is accounted for, is shown in Fig. 3. The alternative case, where leads are excluded provides entirely different shape and magnitude. A surface plot the classical density is shown in Fig. 4. The interaction with phonons is switched off. The carriers injected into the S/D regions from the $y = 0$ boundary are entirely separated by the high barrier and the potential in the substrate. Figure 5 demonstrates a surface plot of the density obtained from the Wigner function. A comparison with the classical density outlines effects

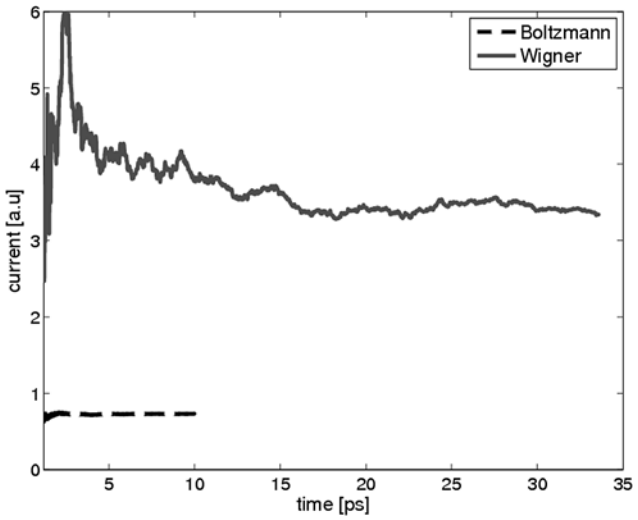

Fig. 6 Convergence of the current

of tunneling and separation. The plot follows the pattern imposed by the potential. In particular, the region below the barrier peak is well pronounced by the lack of carriers; however an increase of the density is seen on both sides of the peak. The behavior bellow the potential peak is in agreement with the charge set back from the interface due to quantum mechanical description of the charge distribution in the triangular well. This, as already observed both theoretically and experimentally, can lead to effective oxide thickness increase and transconductance degradation in Si-MOSFET's. The density is calculated on a regular, 0.25 nm mesh. The corresponding Wigner function is comprised of more than 16×10^6 phase space elements. Because of the large number of particles the convergence is reached after 15 days CPU time on a regular 1 GB RAM, 2.5 GHz processor PC.

Figure 6 demonstrates the convergence of the quantum current as a function of the evolution time. The classical current is smaller than the quantum counterpart since the source to drain tunneling.

3 Conclusions

The above results merely demonstrate that 2D Wigner simulations are not an impossible computational task. The Wigner function, which is multi-dimensional and can not be treated deterministically is computed by the stochastic approach at consecutive time steps by updating an array of integers. The approach is still in its infancy: many issues like dependence of convergence on numerical parameters, and choice of appropriate methods for normalization of the computed averages must be explored by a comparison with an independent quantum simulator. The presented approach can not be a challenge to the well established deterministic methods to coherent transport in 2D devices. It is however the core of a general particle scheme which to be able to handle the general case of 2D quantum transport with dissipation. The experience with 1D simulations shows that phonons merely improve the stochastic convergence. Moreover the approach offers a seamless transition between classical and quantum domains, which can be used to reduce the numerical efforts by an intelligent separation of the device into Boltzmann/Wigner domains. Finally MPI and GRID technologies can be easily implemented due to the stochastic nature of the model.

Acknowledgements This work has been supported by the Österreichische Forschungsgemeinschaft (ÖFG), Project MOEL239.

References

1. Kluksdahl, N.C., Kriman, A.M., Ferry, D.K., Ringhofer, C.: Phys. Rev. B **39**, 7720 (1989)
2. Shifren, L., Ringhofer, C., Ferry, D.K.: IEEE Trans. Electron. Devices **50**, 769 (2003)
3. Nedjalkov, M., Kosina, H., Selberherr, S., Ringhofer, C., Ferry, D.K.: Phys. Rev. B **70**, 115319 (2004)
4. Querlioz, D., Saint-Martin, J., Do, V., Bournel, A., Dolfus, P.: In: Int. Electron. Devices Meet., pp. 1–4 (2006). ISBN: 1-4244-0439-8
5. Zaccaria, R., Rossi, F.: Phys. Rev. B **67**, 113311 (2003)
6. Ferrari, G., Bordone, P., Jacoboni, C.: Phys. Let. A **356**, 371 (2006)